Review article

Echocardiographic evaluation of the right atrial size and function: Relevance for clinical practice

Zhen-Yun Sun [a], Qiao Li [b,*], Jun Li [a], Ming-Wei Zhang [b], Ling Zhu [b], Jing Geng [b]

[a] *Department of Diagnostic Ultrasound, Shandong First Medical University & Shandong Academy of Medical Sciences, China*
[b] *Shandong Provincial Hospital Affiliated to Shandong First Medical University, Jinan 250021, China*

ARTICLE INFO

ABSTRACT

Right atrial (RA) structural and functional evaluations have recently emerged as powerful biomarkers for adverse events in various cardiovascular conditions. Quantitative analysis of the right atrium, usually performed with volume changes or speckle-tracking echocardiography (STE), has markedly changed our understanding of RA function and remodeling. Knowledge of reference echocardiographic values and measurement methods of RA volumes and myocardial function is a prerequisite to introduce RA quantitation in the clinical routine. This review describes the methodology, benefits and pitfalls of measuring RA size and function by echocardiography based on the current understanding of right atrial anatomy and physiological function and provides the current knowledge of right atrial function in related cardiac diseases.

1. Introduction

Various anatomical, physiological, electrophysiological and pathological features of the Right atrial (RA) are recognized as unique. RA enlargement and/or dysfunction are increasingly recognized as important predictors of adverse cardiovascular events. Distinguishing between normal and abnormal RA size and function is therefore clinically relevant. In this article, we provide a comprehensive overview of the assessment of RA size and function (Fig. 1) and pressure estimation using echocardiography and a summary of their demonstrated diagnostic and prognostic value.

2. Anatomy of the right atrium

The right atrium of the human heart is situated behind the right ventricle in a rightward direction. It comprises the following parts—a venous component, an appendage, and a vestibule. The main body of the right atrium has an irregular ellipsoid shape with a triangular protrusion of the right atrial appendage from the anterolateral part [1,2]. The interatrial septum is the part common for both atria, and it is oriented obliquely anteriorly to posteriorly rightward at an angle of approximately 65° to the sagittal plane [3,4].

Characteristic of the right atrium is the crista terminalis visible on the endocardial surface. The crista terminalis is the muscle bundle that delineates the border between the smooth wall of the venous component and rough wall of the appendage. It extends from the left side of the superior vena cava ostium, passes just in front of it, travels down laterally curving to the right of the inferior vena cava (IVC) and finally ends by ramifying in the area between the ICV and tricuspid valve (the cavotricuspid isthmus) [1,5]. Myocytes in the crista terminalis are mostly aligned along the long axis of the muscle bundle, favoring preferential conduction. However, myofibers in the intercaval area, outside the crista terminalis, are aligned obliquely. This abrupt change in orientation represents an ideal substrate for atrial arrhythmia [6,7].

Koch's triangle, which is the part of the vestibule of the RA, is considered as an anatomic landmark for the localisation of the right atrioventricular (AV) node. Its apex is located in the central fibrous body and is the site of penetration of the bundle of His, while its base is

described as the line segment tangent to the left border of the coronary sinus ostium between the left end of the Eustachian ridge and the tricuspid annulus (TA). The anterior edge of the triangle stretches between the apex and the point where the base touches the TA. The posterior edge extends between the apex and the point where the base reaches left end of the Eustachian ridge [8].The AV node is found mainly at the Koch's triangle apex [9]. Knowledge of Koch's triangle dimensions is extremely important to safely perform radio-frequency catheter ablation within the RA because unwanted ablation of the AV node inside Koch's triangle may result in nodal injury and complete block of conduction. On the other hand, the area of Koch's triangle is related to the pathophysiology of AV nodal re-entrant tachycardias. Hence, the
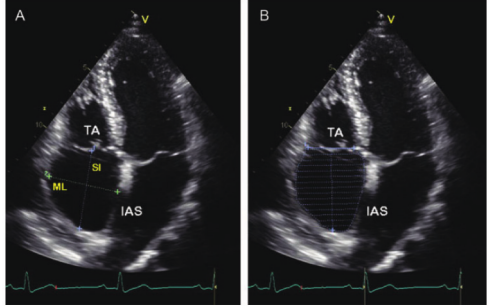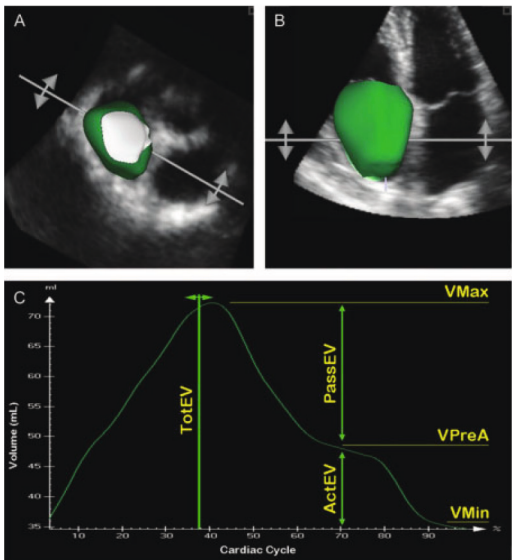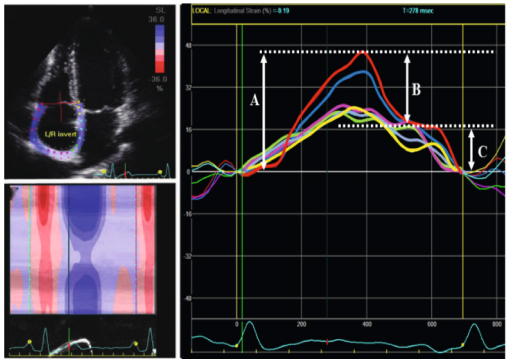
RA size and function	Technique
(A) RA supero-inferior (SI) and medio-lateral (ML) diameters (B) RA area tracing. IAS, interatrial septum; TA, tricuspid annulus.	- Optimize the right atrium (RA) by acquiring dedicated, non-foreshortened apical 4-chamber views in which RA cavity is maximized both longitudinally and transversally - Circumference was drawn from lateral to septal border of the tricuspid annulus, excluding the area between tricuspid leaflets and annulus, along RA endocardium, excluding Vena cava inferior/Vena cava superior and RA appendage. Measured RA area and volume at end-systole. - Biplane disc summation method is recommended for RA volume calculation. - RA volumes should be indexed to body surface area.
	- Optimize RA image quality, adjust probe position for a complete visualization of RA contour in all views throughout the cardiac cycle. - Optimize temporal resolution, whenever feasible, obtain a multi-beat acquisition to maximize frame-rate. - From this time – volume curve, the values for Vmax, Vmin, and VpreA RA volumes can be obtained. - Parameters of phasic RA function (active and passive emptying volume and fraction and) are calculated from these volumes.
A = RA reservoir function; B = conduit function; C = contractile function.	Longitudinal Strain - Obtain unzoomed RA focused and optimized view. - Acquire 3-5 cardiac cycles at high frame rates (>55fps). - Optimize 2D image quality. - A：peak positive longitudinal strain in systole - B : longitudinal strain in early diastole - C: longitudinal strain in late diastole

Fig. 1. Overview of the various parameters employed to assess RA size and function using contemporary echocardiography [24].

musculature located in the apex of the Koch's triangle is not the target for ablation of the so-called fast pathway [10].

3. Physiological function of the right atrium

Physiologically, the right atrium contributes to pulmonary hemodynamics by modulating right ventricular filling through the interplay of 3 main phases: 1) The reservoir phase, which acts as a "reservoir" for systemic blood after tricuspid valve (TV) closure. This phase depends on right ventricular (RV) longitudinal contraction, right atrium compliance and caval venous return. An increase in this phase helps to increase RV filling. 2) The conduit phase acts as a "conduit" for passive filling of the vena cava after opening the TV. This phase is dependent on aging and RV diastolic function. 3) The active contraction phase (when sinus rhythm (SR) is present) acts as a "booster pump" for end-diastolic atrial contraction to promote RV filling. This phase is dependent on atrial wall contractile properties and ventricular end diastolic pressure.

4. RA size

Two-dimensional (2DE) and three-dimensional (3DE) echocardiography are the most commonly employed noninvasive imaging techniques to evaluate RA size [11–13]. Volumetric assessment of the RA size may be more accurate than linear measurement because RA enlargement is asymmetrical. Current American Society of Echocardiography (ASE)/European Association of Cardiovascular Imaging (EACVI) Recommendations suggest assessing RA volume in daily clinical practice by 2DE using single plane area-length or the method of disks in a dedicated apical four-chamber view [14].

Keller et al. [15] found higher absolute sex-specific RA mean volume normal values of 46.9 ml in men and 33.6 ml in women. Lang et al. [14] reported RA volume normal values normalized for BSA of 21 ml/m^2 in women and 25 ml/m^2 in men. Body size is a determinant of RA size, and absolute RA volumes are larger in men than in women; indexation to body surface area (BSA) and height corrects for the effect of sex [14,15]. No significant age-related differences in 2D RAV measurements were found for either sex. Considerable geographic variations in RA size and function were identified. Asian individuals of both sexes had significantly lower BSA than non-Asian individuals, and their 2D and three-dimensional (3D) end-systolic RA volumes were significantly smaller even after BSA indexing [16,17].In addition to sex and age, multivariable regression identified body mass index, coronary artery disease, chronic heart failure and atrial fibrillation (AF) as independent key correlates of the RA volume in both sexes [15].

Two-dimensional echocardiography evaluates right atrial size and estimates the volume by making geometric assumptions. This approach entails limitations in assessing the size of nonspherical atria. Additionally, errors due to foreshortening and off-axis image planes are inherent to 2DE. Despite these limitations, 2D parameters can be easily measured and are an important part of echocardiographic assessment to obtain a fast and simple impression of RA deviation.

3DE has many advantages over 2DE, such as the following: (1) improved visualization of the complex shapes and spatial relationships between cardiac structures; (2) improved quantification of cardiac volumes and function; and (3) improved display and assessment of valve dysfunction [18–20]. Using current 3DE technology (Fig. 1), real-time three-dimensional imaging enables the acquisition of narrow pyramidal datasets in a single heartbeat [21]. The availability of single-beat acquisitions allows reliable RA 3DE quantification even in patients with AF. Both semiautomated and fully automated contour detection algorithms have good correlations with manual tracing, with significant reduction in the analysis time and improved reproducibility [22]. The major limitations at present are the limited spatial resolution of 3DE data sets and the paucity of data for both normative values, as well as prognostic value of 3DE RA volumes and phasic function indices.

Several studies have shown that 3DE RA phasic volumes are significantly larger than those calculated using 2DE [22–24](Table 1). Peluso et al. [24] showed that indexed 3D volumes were significantly larger in men than in women, suggesting the need for sex-specific reference values. 3D RAV values differed minimally with age, remaining significant after BSA indexing.

4.1. Take-home messages

4.1.1. Linear dimensions

Strengths: Easy to obtain and established normal values.
Weaknesses: Single dimension only and assumes that RA enlargement is symmetrical.

4.1.2. 2DE RA volumes

Strengths: Easy to perform, widely available, do not require specific software, with a large body of both normative data and data demonstrating prognostic value in various cardiac conditions.
Weaknesses: Underestimate the actual RA volume, needs dedicated RA views, depends on geometric assumptions for volume calculations, and interobserver variability and repeatability are less optimal.

4.1.3. 3DE RA volumes

Strengths: No geometric assumptions and therefore more accurate volumes, can be used in AF, less interobserver variability and less analysis time, ideal for serial measurements.
Weaknesses: Poor spatial resolution, require specific transducer for image acquisition and particular software for measurements, and lack of supporting normative and prognostic data.

5. RA pressures

Right atrial pressure (RAP) is a hemodynamic variable that provides crucial diagnostic and prognostic information in both cardiovascular and pulmonary disease patients [25–29]. Reference standard RAP is measured employing right heart catheterization, but right heart catheterization is unsuitable for regular serial assessment.

Previous echocardiographic methods to noninvasively determine RAP include 2DE, Doppler, and tissue Doppler imaging (TDI) methods. Additionally, myocardial deformation imaging has recently developed and was proven to be an accurate indirect means to estimate RA pressure.

Existing 2DE estimation methods center on IVC size and its collapse following inspiration (Fig. 2). Current guidelines recommend estimating right atrial pressure by the 3–8–15 mm Hg method [14]. In this approach, the RAP is 3 mm Hg if the IVC diameter is ≤21 mm and the diameter changes ≥50 % with sniffing; the RAP is 15 mm Hg if the IVC diameter is >21 mm and the diameter changes <50 % with sniffing; if

Table 1
Comparison between 3DE and 2DE parameters of RA size and function [24].

Right atrial parameter	RA size		
	3DE	2DE	P-value
Maximal volume (ml)	52 ± 15	41 ± 14	<0.0001
Minimal volume (ml)	19 ± 8	17 ± 7	<0.0001
PreA volume (ml)	28 ± 10	27 ± 11	<0.0001
Total EV (ml)	33 ± 10	24 ± 9	<0.0001
Passive EV (ml)	24 ± 9	14 ± 7	<0.0001
ActEV (ml)	9 ± 4	10 ± 5	0.017
TotEF (%)	63 ± 9	58 ± 9	<0.0001
PassEF (%)	46 ± 11	34 ± 12	<0.0001
ActEF (%)	31 ± 8	35 ± 11	<0.0001

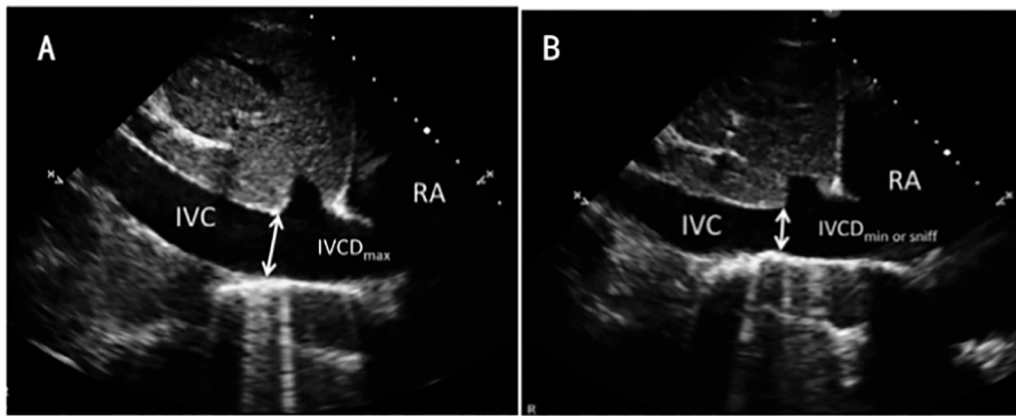EV, emptying volume; EF, emptying fraction;

Fig. 2. Cross-sectional echocardiograms of the IVC in the subcostal long-axis view at end-expiration (A) and during inspiration with or without sniff (B). RAP was estimated by the respirophasic variation of the inferior vena cava diameter (IVCD) [30].

neither condition is satisfied, the RAP is 8 mm Hg. Body size, measured as BSA, must be considered when the IVC diameter is used to assess RAP [30,31]. Taniguchi et al.[30] found that the optimal cutoff point of the maximal IVC diameter was 21 mm for patients with a larger BSA and 17 mm for those with a smaller BSA. However, the cutoff point of IVC collapsibility was not influenced by the difference in BSA. It should be noted that in normal young athletes, the IVC may be dilated in the presence of normal pressure [14]. In addition, the IVC is commonly dilated and may not collapse in patients on ventilators, so it should not be routinely used in such cases to estimate RA pressure.

Estimated RA pressure based on IVC size and collapsibility has fairly good correlations with invasively measured RA pressure, but there are wide limits of variation around the regression line in many studies limiting the utility in individual patients. Recently, the use of Superior vena cava (SVC) flow evaluation from the subcostal window for estimating RAP was recommended in the ASE guidelines [32]. RAP was inversely correlated with the ratio of peak systolic to diastolic forward SVC flows (SVC-S/D) (r = −0.50, P < 0.001), and was an independent determinant of SVC-S/D after the adjustment for right ventricular systolic function (β = −0.48, P < 0.001) [33]. A cutoff value of 1.9 for SVC-S/D showed 85 % sensitivity and 74 % specificity in identifying elevated RAP. Additionally, SVC-S/D showed an incremental diagnostic value combined with inferior vena cava size and collapsibility (P = 0.006) [33]. Hence, the use of SVC flow may be an alternative to IVC parameters for RAP estimation in individuals in whom the IVC appears enlarged despite low RAP.

The parameters for assessing RAP by Doppler and TDI methods

included tricuspid E/e′ (Fig. 3), E′, A′ and E/A. The RV E/e′ ratio, which reflects the right ventricular filling pressure, is a surrogate of RAP [14]. When RV relaxation, compliance and filling pressures are normal, normal myocardial function results in normal lateral e′ velocity, while normal/low RAP results in low trans-tricuspid E velocity; the ratio between E and e′ is therefore low. However, when RV diastolic function is impaired and filling pressures are increased, e′ velocities are reduced because of impaired myocardial relaxation, while elevated RAP drives a higher trans-tricuspid E velocity; the ratio between E and e′ is therefore increased. Utsunomiya et al. [34] found that in 50 patients with a range of etiologies of PH, an RV-E/e′ > 7.3 predicted mRAP>10 mm Hg with 87 % sensitivity and 97 % specificity. Hayabuchi et al. [35] found no significant correlation between RV-E/e′ and mRAP in 25 asymptomatic pediatric repaired Tetralogy of Fallot patients. Tsutsui et al. [36] found a weak correlation between RV-E/e′ and RAP in a group of 71 patients with acute decompensated heart failure(HF). In summary, several studies involving PH or advanced HF/transplantation populations have compared invasively measured RAP with RV-E/e′ estimated RAP. The results showed a reasonable diagnostic ability of RV-E/e′ for estimating RAP in patients with coronary artery disease and RV systolic dysfunction [34,37–39]. The diagnostic ability of RV-E/e′ was generally poor in studies of pediatrics, heart failure and mitral stenosis [35,36,40], while the results were equivocal in other diseases [41]. Bland–Altman analyses showed good accuracy but poor precision of RV-E/e′ for estimating RAP [34,36]. This finding suggests that RV-E/e′ may be useful at a population level but not at an individual level for clinical decision-making.

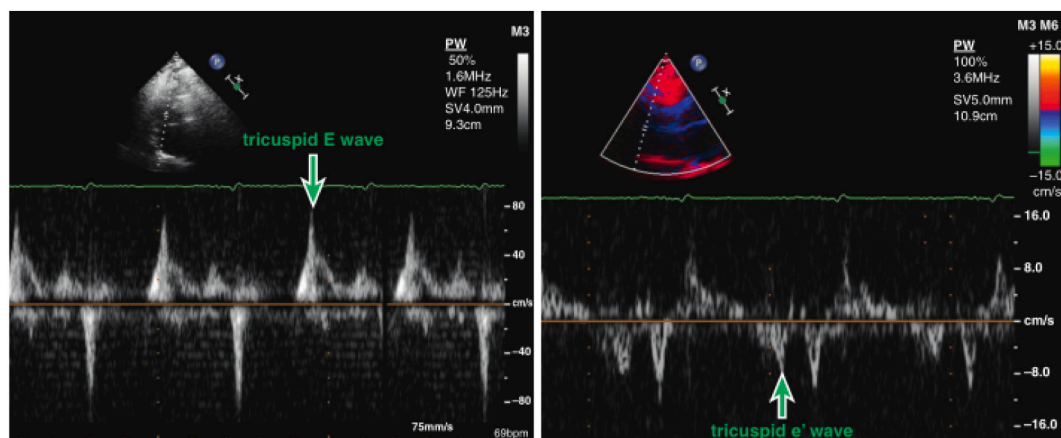In 23 patients with PH and 20 patients with left heart failure,

Fig. 3. In patients in sinus rhythm, RAP was estimated by using the ratio of early tricuspid inflow and early diastolic tissue Doppler tricuspid annular velocities (E/e′) [37].

Watanabe et al. [28] evaluated five parameters, tricuspid E/A, E′, A′, and E/e′, and the respirophasic variation of the inferior vena cava diameter. They found that A′ was the most significant independent predictor of catheterization-based RAP in patients with PH. In patients with left heart failure, catheterization-based RAP was not correlated with any of the 5 echocardiographic parameters. In addition, severe tricuspid regurgitation and tricuspid annular descent may affect these variables including tricuspid E/e′, E′, A′ and E/A, which reduces the clinical utility of these parameters in assessing individual patients.

Studies have also investigated associations between the RA size and invasive RAP (RAP$_{Invasive}$) employing both 2DE and 3DE. RA size assessment offers supportive evidence and may be of additional value to identify elevated RAP. Ellen et al.'s [42] study showed that RA volume assessed with 2DE or 3DE, as well as the RA area, has a better discriminatory ability to detect mRAP above 8 mm Hg than either IVC diameter or collapsibility in patients evaluated for PH. The optimal threshold was 57 ml/m^2 for 3DE RAVmax and 36 ml/m^2 for 2DE RAVmax.

5.1. Take-home messages

5.1.1. RA pressure estimates

Strengths: All spectral Doppler and RA deformation markers are fairly accurate in predicting raised (>15 mm Hg) RA pressure. Weaknesses: They are indirect measures based on pressure difference between RA and RV. All predictors of raised RA pressure should be taken in combination and in the context of increased RA volume.

6. RA function

6.1. Volumetric parameters of RA function

Phasic RA volumes are calculated by measuring RA volumes at various times of the cardiac cycle (Table 1): RA maximal volume (V$_{max}$) is measured before TV opening, pre-A RA volume (V$_{PreA}$) at the beginning of the P wave on the electrocardiogram, and RA minimal volume (V$_{min}$) at the end of diastole (before TV closure). Using the RA volumes, researchers calculated the total emptying volume (TotEV), which represents the RA reservoir function, as the difference between V$_{max}$ and V$_{min}$; passive EV (PassEV), which represents conduit function, as the difference between V$_{max}$ and V$_{preA}$; and active EV (ActEV), which corresponds to RA booster function, as the difference between V$_{preA}$ and V$_{min}$ [24,43]. Accordingly, the total emptying fraction (TotEF) was TotEV/V$_{max}$, the passive EF (PassEF) was PassEV/V$_{max}$, and the active EF (ActEF) was ActEV/V$_{preA}$ [24,43].

Theoretically, 2D echocardiography-based volumetric measurements are possible using RA area and length data. 2DE calculation of RA phasic volumes is time-consuming and prone to error because of the need for three manual endocardial tracings of RA volumes at three different phases of the cardiac cycle and limitation of geometric assumptions concerning atrial shape. 3DE overcomes these limitations, making the assessment of RA phasic volumes and function parameters accurate and reproducible and less time-consuming (the endocardial surface is automatically mapped by the algorithm) [22]. Reference values of RA phasic function, measured by 3DE, have been reported. TotEV, PassEV, TotEF, and PassEF obtained using 2DE were lower than those obtained using 3DE [24,43] (Table 1).

Reference values for RA phasic function should be sex- and age-specific [24,43]. Three-dimensional echocardiography RA TotEV, PassEV, and ActEV were higher in men, but these differences disappeared after indexing for BSA. However , the 3DE RA TotEF, PassEF, and ActEF were higher in women. TotEV did not change significantly with age, but PassEV decreased and ActEV increased with age in both sexes. Similarly, PassEF decreased with age, and ActEF increased with a mild decrease in TotEF in both sexes [24]. These results are consistent with the

documented age-related decrease in the tricuspid valve E/A ratio.

6.1.1. Take-home messages

6.1.1.1. 2DE volumetric phasic RA volumes.

Strengths: Do not require specific software, with a large body of supporting data.

Weaknesses: Three separate manual tracings are required thereby increasing errors, need focused RA views, geometric assumptions for volume estimation, large interobserver and test/retest variability.

6.1.1.2. 3DE volumetric phasic RA volumes.

Strengths: Fully or semiautomated endocardial border tracings, less interobserver variability and less analysis time.

Weaknesses: Require proprietary software packages, increased costs, and others as mentioned in 3DE RA volumes.

6.2. Doppler parameter of RA function

The concept of the "atrial function index" was originally proposed in 2002 by Thomaset et al. [44] in patients with left-sided systolic heart failure and is calculated as a ratio, including analogs of left atrial reservoir function and size, as well as cardiac output. Following the left heart failure paradigm, Sophia et al. [45] explored the prognostic significance of the RA function index (RAFi). RAFi was calculated as (RA emptying fraction × right ventricular outflow tract velocity-time integral)/(RA end-systolic volume index) (as shown in Fig. 4).They found that RAFi was related to 6-minute walk distance (r = 0.37, P = 0.01), while it showed a stronger negative correlation with NTproBNP (r = 0.62, P < 0.0001) and was a prognostic marker in patients with pre-capillary PH. ROC analysis demonstrated that the optimal cutoff value of RAFi for predicting death was 5.3 %, with sensitivity of 66.7 % and specificity of 30% [45]. Therefore, RAFI, a simple parameter that reflects the RA size, reservoir function, and cardiac output in patients with precapillary PH, may be more useful in routine clinical care. Further studies are needed to validate RAFi and define its role in clinical practice.

6.2.1. Take-home messages

6.2.1.1. RA function index.

Strengths: Does not require propriety software, can be used in non-sinus rhythm, has functional and prognostic utility.

Weaknesses: Requires multiple parameters to be measured, relatively few of published studies.

6.3. Strain parameters of RA function

Strain represents myocardial deformation, whereas the strain rate represents the speed at which myocardial deformation occurs [46,47]. Strain measurements allow discrimination between active myocardial deformation and passive wall motion and regional or segmental ventricular strain differences can quantify intraventricular dyssynchrony [48,49]. RA myocardial strain parameters obtained using 2D-STE correlate with 3DE phasic volumetric parameters but are less load-dependent [24]. RA strain parameters represent the physiology of atrial function and are also closely related to RV mechanics during the cardiac cycle [50,51].

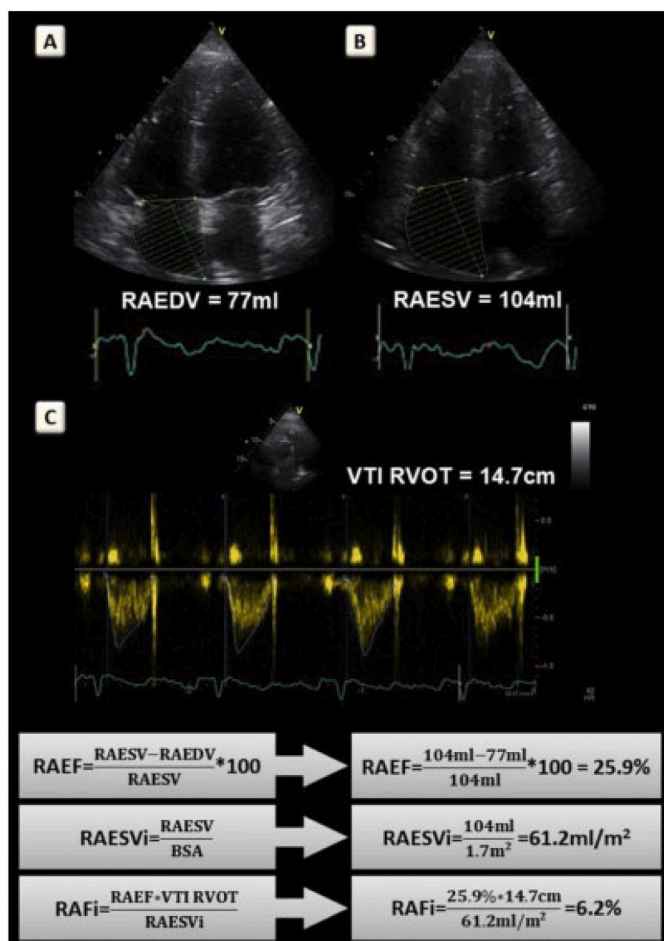Right atrial strain measurements can be obtained by either TDI, 2D-

Fig. 4. Calculation of RAFi. RAFi calculation in a 54-year-old male patient with idiopathic pulmonary arterial hypertension who was under double oral targeted therapy [45]. Right atrial volumes were calculated using the single-plane area-length method from the apical four-chamber views at end-diastole (A) and end-systole (B). The VTI-RVOT was obtained from the parasternal short-axis view (C). BSA, body surface area; RAEDV, RA end-diastolic volume; RAESV, RA end-systolic volume.

STE, or, recently, 3DSTE (Fig. 5). TDI is a robust, easily available, relatively reproducible technique. However, accurate data recording requires a high frame rate, is angle dependent, and is affected by translational movements and tethering [48,49]. Therefore, clinical application is limited. 2DSTE is prominent because of its angle independence compared with TDI, low load dependency compared with volumetric methods in normal subjects, and relative resistance against translational motion [52,53]. With 2D tracking, speckles are lost when they move out of the imaging plane. The principal advantage of 3DSTE over 2DSTE is that speckles can be followed in all directions [48,49].

Strain can be measured in any myocardial plane, but the only recommended strain parameter of RA function is the global longitudinal strain [46]. In contrast to global longitudinal strain measurements, segmental strain measurements continue to have a higher degree of measurement variability between vendors, and test-retest variability is also high [54]. The success of global strain is partly due to the benefit of spatial averaging to control the impact of signal noise; this situation is not available with regional strain. Trying to overcome signal noise with smoothing may lead to a lower sensitivity toward small segments [54]. Therefore, single segmental strain measurements should be used only with great caution [54]. More recently, the usefulness of 3DSTE in assessing RA unidirectional, multidirectional as well as areal strain has been demonstrated [55–59].

Normal range values of RA strain parameters are essential to identify normal and abnormal values, compare them with reference values, and determine the clinical meaning of obtained values. However, significant heterogeneity exists in the reported normal values of RA strain parameters because of the sample size, right atrial volume index (RAVi), sex, heart rate, type of software, and method of global value calculation [53]. The development of a consensus approach by the EACVI/ASE/Industry Task Force to standardize deformation imaging reduced the impact of these differences [46,47].They recently published a consensus document to standardize RA strain analysis and nomenclature by 2DSTE [46]. For standardization purposes, the region of interest is contoured, starting at the tricuspid valve annulus, along the endocardial border of the RA lateral wall, RA roof, RA septal wall, and ending at the opposite TA, and its thickness is reduced to fit the thin RA wall. For adequate tracking, a dedicated RV-focused apical four-chamber view visualizing the entire RA and optimization of the orientation, gain, and depth to obtain nonforeshortened views of RA walls throughout the cardiac cycle is recommended [46].

Padeletti et al. [60] provided the RA function data of 84 healthy individuals. They reported that the RA global strain was 49 ± 13 % in this normal population sample, while the RA strain during late diastole was 18 ± 6.38 %. A meta-analysis of 2469 normal subjects [53] provided more robust reference ranges for RA strain parameters by 2DSTE. The normal range values for RA strain and the strain rate were 42.7 % (95 % CI, 39.4 to 45.9 %) and 2.1 s^{-1} (95 % CI, 2.0 to 2.1 s^{-1}) during the reservoir phase, respectively, 23.6 % (95 % CI, 20.7 to 26.6 %) and -1.9 s^{-1} (95 % CI, -2.2 to -1.7 s^{-1}) during the conduit phase, correspondingly, and 16.1 % (95 % CI, 13.6 to 18.6 %) and -1.8 s^{-1} (95 % CI, -2.0 to -1.5 s^{-1}) during the contraction phase, respectively. Recently, The World Alliance of Societies of Echocardiography has also reported age- and sex normal reference values of RA strain parameters [20] (Table 2). A prospective study [61] provided normal reference values for RA strain parameters derived from 3DSTE and showed different behaviors of RA strains compared with LA strains. RA strains show obvious sex dependency, which could not be confirmed in LA strains [62,63]. However, further studies are needed to confirm these findings and further assess RA strains in different pathological conditions [55–59].

According to some studies, the RA strain during the reservoir and conduit phase were higher in women, while RA strain during late diastole was similar in men and women [53,61]. Female individuals have higher circumferential and areal strain values than men according to 3DSTE [61]. Using 2D or 3DSTE, RA strain parameters reflecting reservoir and conduit functions decrease with age, while reflecting systolic function increases with age [53,61].

6.3.1. Take-home messages

6.3.1.1. Tissue Doppler-derived strain. Not to be used anymore due to suboptimal reproducibility, angle-dependence, signal artifacts and the fact that it only measures regional strain.

6.3.1.2. STE strain.

Strengths: Uses conventional grayscale four-chamber view, easy to perform and highly reproducible, demonstrated prognostic value; dedicated software packages are now available.

Weaknesses: They are currently measured using LV strain packages; intervendor variability not yet assessed, Prognostic value still to be defined in large multicenter studies.
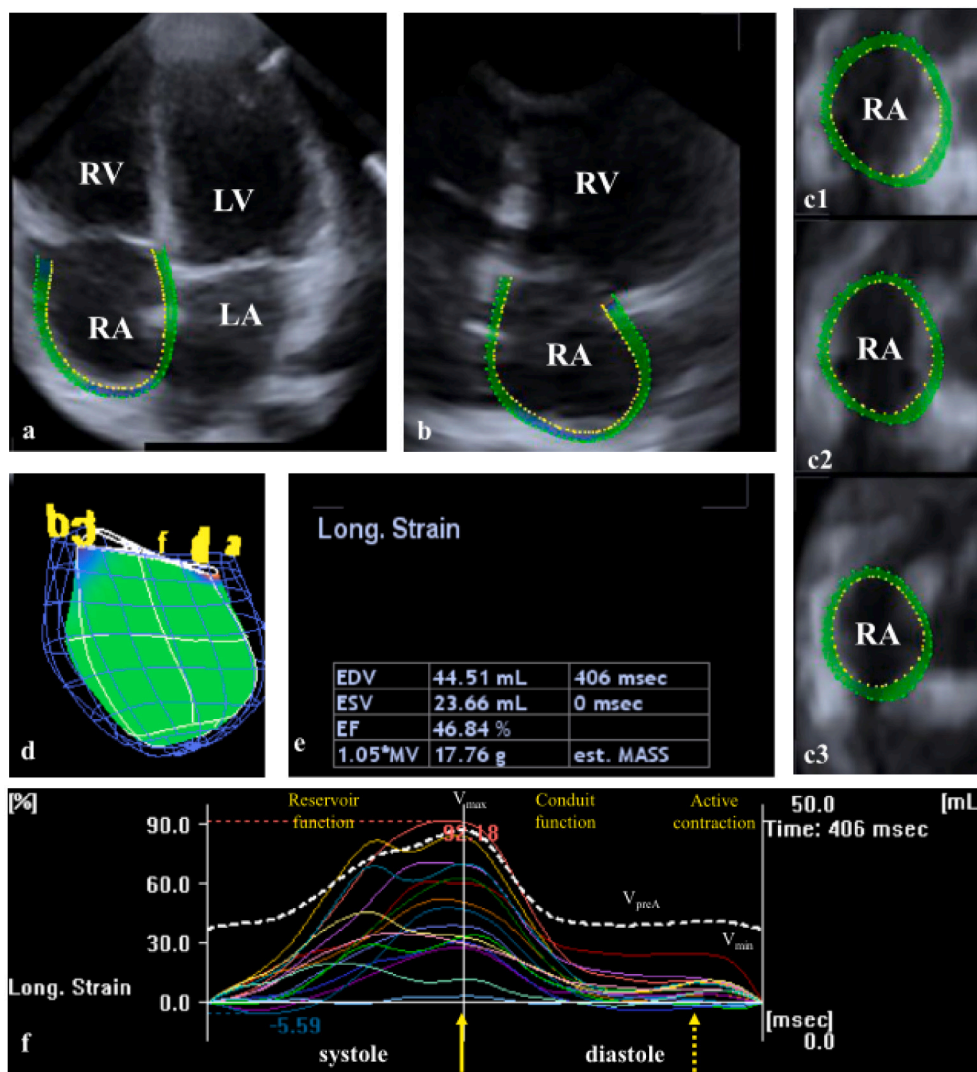
Fig. 5. Images from three-dimensional (3D) full-volume dataset showing the right atrium (RA) in a healthy subject [61] are demonstrated (a, b): a apical four-chamber view, b apical two-chamber view, c1 parasternal short-axis view at basal, c2 mid- and c3 superior RA levels. In d 3D reconstruction of the RA based on 3D speckle tracking echocardiographic analysis is presented. In e RA volumetric data are demonstrated. Colored lines represent segmental RA strains while dashed white line represents RA volume changes over the cardiac cycle (f). Yellow arrow represents peak RA strain, while dashed arrow represents RA strain at atrial contraction.

Table 2
Age-dependency of RA strain parameters are listed for all subjects and for both sexes separately (mean ± 1.96 * SD) [16].

	All Subjects				Males				Females			
	18–40 years (N = 854)	41–65 years (N = 653)	>65 years (N = 501)	P	18–40 years (N = 435)	41–65 years (N = 344)	>65 years (N = 254)	P	18–40 years (N = 419)	41–65 years (N = 309)	>65 years (N = 247)	P
RA reservoir strain (%)	52.3 ± 12.5	41.5 ± 10.7	38.4 ± 10.6	*^#	50.0 ± 11.9	40.9 ± 10.9	38.5 ± 11.5	*^#	54.8 ± 12.7	42.1 ± 10.4	38.4 ± 9.5	*^#
RA conduit strain (%)	−22.5 ± 6.8	−16.2 ± 6.0	−13.2 ± 6.0	*^#	−21.4 ± 6.2	−15.6 ± 6.0	−13.4 ± 6.1	*^#	−23.7 ± 7.3	−16.8 ± 5.9	−12.9 ± 5.9	*^#
RA contractile strain (%)	−30.0 ± 10.2	−25.6 ± 8.5	−25.5 ± 9.1	*^	−28.8 ± 9.4	−25.6 ± 8.8	−25.4 ± 9.4	*^	−31.3 ± 10.9	−25.6 ± 8.2	−25.7 ± 8.9	*^

P: * 18–40 vs 41–65; ^ 18–40 vs >65; # 41–65 vs >65.

7. RA function in common cardiovascular diseases

7.1. Pulmonary hypertension

The relaxation and distensibility of RA and right ventricular systolic function are the most important factors affecting right atrial reservoir function. In the early stage of PH, because of the increased right ventricular systolic function, the passive dilatation of the right atrium is enhanced by right ventricular systolic traction. Although right ventricular systolic function is decreased with disease development, the right atrial myocardium is particularly thin, has strong relaxation and

distensibility, and responds to overload with dilatation rather than hypertrophy, compensating for the effect of decreased right ventricular systolic function on right atrial reservoir function. Therefore, the general trend of RA reservoir function is enhanced [64,65].

In the early stage of pulmonary hypertension, the RA conduit function was decreased because of RV afterload increment, hypertrophy of the RV myocardium, delayed relaxation, decreased diastolic function, and weakened suction of RV active dilation. Decreased RV diastolic function results in decreased RV compliance, an increase in RV diastolic pressure and therefore an increase in RA volume. Clinical studies have revealed that the Frank-Starling mechanism operates in the right atrium

of patients with chronic PH [66,67]. According to this law, the right atrium increases its ejection force, resulting in enhanced active systolic function.

In the early stage of PH, right atrial conduit function decreases, while reservoir and systolic functions increase to maintain cardiac output [64,65,68]. In advanced PH, as RV diastolic dysfunction progresses, patients exhibit pseudonormal or restrictive filling, conduit function increases, and reservoir and systolic functions decrease [69,70]. However, the shift from reservoir to conduit function was inadequate to maintain cardiac output. In Sato and Gaynor's study [71,72], the cardiac output was inversely related to the conduit-to-reservoir ratio, increasing as the reservoir contribution increased (P = 0.03).

Right atrial dilatation and increased RA pressure are associated with adverse outcomes in patients with PH. A recent study [70] showed that clinical deterioration is better associated with right atrial rather than right ventricular remodeling. In a prospective observational study, Fawaz Alenezi et al. [73] found that RA dysfunction, as assessed by the RA reservoir, conduit, and active contraction, is an independent predictor of mortality and hospitalizations in PH. An echocardiographic retrospective study involving 37 patients with PH [74] showed that RA reservoir function, was significantly lower in patients with clinical worsening during follow-up. Sato et al. [75] observed that the RA volume and reservoir function and their combined use with RV are novel predictors of clinical worsening in patients with precapillary PH. A recent study involving 160 patients with different forms of PH (Groups 1 to 5) [76] showed that a decreased RA emptying fraction (calculated as the maximum minus minimum RA volume on cardiac magnetic resonance imaging) is independently associated with worse survival after adjusting for other risk factors. Additionally, right atrial peak atrial longitudinal strain (PALS) is a valuable factor for predicting the functional status and exercise capacity in PH patients. A study with 2DSTE [70] showed that right atrial PALS was significantly lower in PH patients than in controls and gradually reduced with the development of cardiac insufficiency. A significantly positive correlation between global PALS and the 6-minute walk distance was found (P = 0.003).

7.2. Myocardial infarction

The effect of myocardial infarction on right atrial function varies depending on the location of infarction. When right ventricular myocardial infarction occurs, right ventricular diastolic function is reduced, followed by decreased systolic function [77]. Impaired RV diastology and chronic RA pressure overload lead to impaired right atrial compliance and decreased right atrial reservoir and conduit functions. As a compensatory mechanism, RA booster pump function is enhanced to ensure RV filling [78]. Evaluation of right atrial function by 2DSTE in patients with inferior myocardial infarction (INFMI) and patients affected by both INFMI and right ventricular myocardial infarction (RVMI) by Nourian et al. [79] demonstrated that right atrial reservoir and conduit functions were impaired in patients with INFMI and RVMI compared with those with INFMI. Right atrial early diastolic longitudinal strain <27.5 % showed 59.3 % sensitivity and 79.1 % specificity to discriminate INFMI and RVMI from INFMI.

Although acute myocardial infarction mostly comprises ventricular infarction, it can still involve the atria and is not rare. In 1942, Cushing et al. [80] published the clinical data and pathology findings from 182 patients who died because of ventricular myocardial infarction. Atrial infarction was demonstrated in 17 % of the patients: 27 in the right atrium and 4 in the left atrium. In contrast to ventricular infarction, most of the atrial infarctions involve the right atrium versus the left atrium. A review of case series showed that the right atrium is involved in 81 % to 98 % of cases, and the left atrium is involved in only 2 to 19% [81,82]. The considerably higher oxygen content of left atrial blood may explain the difference in incidence between right and left atrial infarction.

7.3. Atrial fibrillation

Histological studies of RA myocardium in AF show the same substrate of patchy fibrosis, inflammatory cell infiltrate, necrosis, and vascular degeneration [83–86], as seen in the left atrium. Similar electrical remodeling with downregulation of L-type calcium currents (Ical) and Ca(2+)-ATPase is also observed in both atria of patients with paroxysmal and persistent AF [87–89]. An electrophysiology study [90] with detailed biatrial electroanatomic mapping has demonstrated that AF is associated with remodeling processes affecting both atria. The observed RA remodeling could be an accurate correlate of LA remodeling [90].

AF causes biatrial enlargement, and the restoration of SR after ablation or cardioversion leads to biatrial reverse remodeling. Akutsu et al. [91] showed an association with RA remodeling, and AF recurrence and the RA and LA volumes (>87 and >97 ml, respectively) were predictive of AF recurrence postcatheter ablation. In a study by Therkelsen et al. [92], only the RA volume was normalized 180 days after cardioversion compared with that in healthy volunteers. This finding may highlight the greater and faster ability of the right atrium to reverse structural remodeling. Using 3DE and strain analysis, Soulat-Dufour et al. [93] evaluated reverse biatrial remodeling in patients with AF who were successfully cardioverted. Remodeling of the structure and function was observed, with a significant decrease in the biatrial 3D volume and a significant improvement in the biatrial global reservoir strain, 3D right atrial emptying fraction and 3D right atrial expansion index. Govindan et al. [94] demonstrated that RA and RV deformation properties are significantly impaired in patients with recurrent AF compared with those who maintain SR for up to 12 months, and a higher RA booster strain independently predicted SR maintenance for up to 12 months.

Additionally, RA dysfunction may cause postoperative atrial fibrillation (POAF) development. A study of 142 consecutive patients undergoing coronary artery bypass surgery [95] found that RA dilatation and remodeling were involved in the development of POAF, and the screening of RA functions before surgery may be useful for preventing AF development. Aksu et al. [95] demonstrated that RAVi and right atrial strain during the reservoir phase were independent predictors of AF development and recommended using RAVi for predicting POAF development.

7.4. Atrial functional tricuspid regurgitation

Functional tricuspid regurgitation (FTR) has been considered to be secondary to TA dilation and leaflet tethering, associated to RV dilation and/or dysfunction (the "classical", ventricular form of FTR, V-FTR) for a long time. Atrial FTR (A-FTR) has recently emerged as a distinct pathophysiological entity. A-FTR typically occurs in patients with persistent/permanent AF, in whom the main mechanisms leading to regurgitation are supposed to be the dilation and the decrease of the sphincter-like function of the TA, associated to a dilation of the right atrium and an imbalance in the ratio between TA and leaflet areas [96–98].

The tricuspid valve is a complex structure that includes the TA, the TV leaflets, and a sub-valvular apparatus (chordae and papillary muscles). The healthy TA has a dynamic, 3D saddle-shaped elliptical geometry [99–102], characterized by higher antero-septal and postero-lateral parts and lower antero-lateral and postero-septal parts [102]. Both the anatomic integrity of the TV apparatus and the normal shape and function of the right heart chambers are needed for the correct functioning of the valve [99,100,103].

The size of the TA is larger during diastole and smaller during systole. In pathological conditions of TA dilation, it tends to become more planar and circular [99]. The anterior and posterior parts of the TA are muscular, whereas the septal part is more fibrous. Consequently, the portion of the TA that is the least involved in the remodeling process is

the septal one, the dilation mostly occurring in the antero-posterior direction, and leading to the progressive distancing of the aortic valve and the antero-posterior commissure [99].

Several studies have elegantly described the pathophysiological mechanisms of A-FTR (previously-referred to as "idiopathic" or "isolated" TR). A-FTR is characterized by TA remodeling associated with RA enlargement, and normal/mildly abnormal RV size and function, especially in the initial stages of the disease [104]. Yamasaki et al. [105] hypothesized that severe A-FTR is caused by the loss of systolic leaflet coaptation due to the TA dilation associated with RA enlargement. Muraru et al. [97,106] demonstrated that AF may cause FTR by affecting the geometry of the TA through the remodeling of the RA. Guta et al. [96] have further contributed to understanding the pathophysiology of A-FTR by showing that RA minimum volume is the main determinant of TA area at end-diastole in AF patients, and that it determines A-FTR severity, while leaflet tethering plays a far less important role in the process. Furthermore, Utsunomiya et al. [107] reported that TA area was more closely correlated with RA maximum volume than with RV end-systolic volume in AF patients, and that the only predictor of A-FTR severity was TA area at mid-systole. In contrast, Najib et al. [108] showed that both RA and RV volumes were independent predictors of the development of severe FTR in AF patients. RV enlargement is usually detected in more advanced stages of A-FTR, with longer disease progression, as the dilation of the RV is usually a late event in A-FTR, as reported by Nemoto et al. [109].

However, TA dilation secondary to RA remodeling in patients with persistent/permanent AF is not always associated with the development of significant FTR, and with the same extent of RA and TA dilation, different degrees of FTR may be observed [110]. This may be related to differential TV leaflet remodeling, similar to that described in V-FTR [111,112]. Afilalo et al. [111] demonstrated that in V-FTR, TV leaflets remodel by increasing their area and that both the occurrence and severity of FTR are related to the extent of leaflet adaptation to increased TA area expressed as TV leaflet area-to-closure area ratio. The difference between the extent of TV leaflet areas adaptation in response to TA and RA dilation could be a key factor in the pathophysiological cascade that leads to the development and progression of A-FTR. Moreover, Utsunomiya et al. [113] showed that the posterior dilation of the RA that causes posterior TV plane displacement is not efficiently compensated by the TV leaflet adaptation. These mechanisms might explain why despite similar extent of RA dilation, some of the patients present with only trivial/mild A-FTR [96].

Although still under development and underused in clinical practice, TV interventions should be considered in patients with severe symptomatic FTR, in the absence of severe left ventricular or RV dysfunction, or severe PH [114,115], and In a recent study, patients with severe FTR treated with the transcatheter tricuspid valve interventions had better 1 year prognosis compared to patients undergoing only medical treatment [116]. According to current guidelines [117,118], RV dilation is a criterion for severe FTR. However, Florescu et al. [119] found that patients with severe A-FTR may have normal RV size, or on the contrary, patients with less than severe FTR might have dilated RV. Accordingly, in A-FTR the absence of RV dilation should not be considered an indicator of milder degrees of FTR. Moreover, FTR severity is not linearly associated with prognosis [120], demonstrating that the recommended indications for TV interventions should take into consideration the etiology of FTR [117]. Wang et al. [121] demonstrated that catheter ablation (CA) for AF and SR maintenance lead to TR improvement in FTR patients without significant TV tethering (tethering height < 6 mm). Itakura et al. [122] showed how the reduction in RA size following the restoration of SR by CA correlated with the decrease in FTR severity in patients with persistent AF. However, although cardioversion and/or ablation of AF might be beneficial in patients with A-FTR, these therapies should not delay the referral for intervention in patients with indications [117].

8. Conclusion

RA measurements have been limited to evaluating the RA size, whose assessment may be limited by load dependence and geometric assumptions. Additionally, right atrial dysfunction may be detected in patients with a normal right atrial size. However, various echocardiographic parameters of RA function have been proven to be valuable predictors of early cardiac impairment, primarily in patients with RV pressure and/or volume overload. Emerging data support the role of phasic RA volumes and RA phasic function, utilizing strain analysis. How and when to incorporate these various indices of RA function into clinical practice remains uncertain. While more comprehensive normative data and robust evidence of the prognostic usefulness of the newer techniques, including 3DE and strain analysis, are warranted, evaluating not only the RA volume but also RA function parameters will be included in future guidelines to assess patients.

Ethical statement

This article is a review that does not involve any animals or ethics.

Declaration of competing interest

The authors declare that they have no known competing financial interests or personal relationships that could have appeared to influence the work reported in this paper.

Acknowledgments

References

[1] I. Kucybala, K. Ciuk, W. Klimek-Piotrowska, Clinical anatomy of human heart atria and interatrial septum - anatomical basis for interventional cardiologists and electrocardiologists. Part 1: right atrium and interatrial septum, Kardiol. Pol. 76 (3) (2018) 499–509.

[2] R.M. Kiedrowicz, M. Wielusinski, A. Wojtarowicz, J. Kazmierczak, Left and right atrial appendage functional features as predictors for voltage-defined left atrial remodelling in patients with long-standing persistent atrial fibrillation, Heart Vessel. 36 (6) (2021) 853–862.

[3] B. Jensen, T. Wang, A.F.M. Moorman, Evolution and development of the atrial septum, Anat. Rec. (Hoboken) 302 (1) (2019) 32–48.

[4] N. Naqvi, K.P. McCarthy, S.Y. Ho, Anatomy of the atrial septum and interatrial communications, J. Thorac. Dis. 10 (Suppl 24) (2018) S2837–S2847.

[5] A.U. Siddiqui, S.R. Daimi, K.R. Gandhi, et al., Crista terminalis, musculi pectinati, and taenia sagittalis: anatomical observations and applied significance, ISRN Anat. 2013 (2013), 803853.

[6] G.M. Morris, L. Segan, G. Wong, et al., Atrial tachycardia arising from the crista terminalis, detailed electrophysiological features and long-term ablation outcomes, JACC Clin. Electrophysiol. 5 (4) (2019) 448–458.

[7] Y. Turkmen, P. Insulander, H. Bastani, et al., Focal atrial tachycardia-the localization differences between men and women: a study of 487 consecutive patients, Anatol. J. Cardiol. 24 (6) (2020) 405–409.

[8] J.T. Tretter, D.E. Spicer, D. Sanchez-Quintana, E. Back Sternick, J. Farre, R. H. Anderson, Miniseries 1-part III: 'behind the scenes' in the triangle of Koch, Europace 24 (3) (2022) 455–463.

[9] D. Sanchez-Quintana, R.H. Anderson, J.T. Tretter, J.A. Cabrera, E.B. Sternick, J. Farre, Anatomy of the conduction tissues 100 years on: what have we learned? Heart 108 (18) (2022) 1430–1437.

[10] C. Garweg, S. De Buck, B. Vandenberk, R. Willems, J. Ector, High-detailed evaluation of the right atrial anatomy by three-dimensional rotational angiography during ablation procedures for atrioventricular nodal reentrant tachycardia and atrial flutter, Scand. Cardiovasc. J. 52 (5) (2018) 268–274.

[11] M.H. Lerchbaumer, M. Ebner, C.O. Ritter, et al., Prognostic value of right atrial dilation in patients with pulmonary embolism, ERJ Open Res. 7 (2) (2021).

[12] B.S. Frank, M. Schafer, T.M. Thomas, D.D. Ivy, P.N. Jone, Longitudinal assessment of right atrial conduit fraction provides additional insight to predict adverse events in pediatric pulmonary hypertension, Int. J. Cardiol. 329 (2021) 242–245.

[13] M. Naseem, S. Samir, Right atrial volume index as a predictor of persistent right ventricular dysfunction in patients with acute inferior myocardial infarction and

proximal right coronary artery occlusion treated with primary percutaneous coronary intervention, J. Saudi Heart Assoc. 32 (4) (2020) 500–508.

[14] R.M. Lang, L.P. Badano, V. Mor-Avi, et al., Recommendations for cardiac chamber quantification by echocardiography in adults: an update from the American Society of Echocardiography and the European Association of Cardiovascular Imaging, J. Am. Soc. Echocardiogr. 28 (1) (2015) 1–39, e14.

[15] K. Keller, C. Sinning, A. Schulz, et al., Right atrium size in the general population, Sci. Rep. 11 (1) (2021) 22523.

[16] L. Soulat-Dufour, K. Addetia, T. Miyoshi, et al., Normal values of right atrial size and function according to age, sex, and ethnicity: results of the world alliance societies of echocardiography study, J. Am. Soc. Echocardiogr. 34 (3) (2021) 286–300.

[17] T. Miyoshi, H. Tanaka, Standardization of normal values for cardiac chamber size in echocardiography, J. Med. Ultrason. (2001) 49 (1) (2022) 21–33.

[18] K. Cagli, Z. Golbasi, M. Ozdemir, 3D echocardiographic imaging of an extremely rare rotation anomaly of the heart, J. Echocardiogr. 17 (4) (2019) 213–214.

[19] T. Kimura, V.L. Roger, N. Watanabe, et al., The unique mechanism of functional mitral regurgitation in acute myocardial infarction: a prospective dynamic 4D quantitative echocardiographic study, Eur. Heart J. Cardiovasc. Imaging 20 (4) (2019) 396–406.

[20] D. Muraru, R.T. Hahn, O.I. Soliman, F.F. Faletra, C. Basso, L.P. Badano, 3-dimensional echocardiography in imaging the tricuspid valve, JACC Cardiovasc. Imaging 12 (3) (2019) 500–515.

[21] K. Tanabe, K. Yamaguchi, Incorporating three-dimensional echocardiography into clinical practice, J. Echocardiogr. 17 (4) (2019) 169–176.

[22] E. Aune, M. Baekkevar, J. Roislien, O. Rodevand, J.E. Otterstad, Normal reference ranges for left and right atrial volume indexes and ejection fractions obtained with real-time three-dimensional echocardiography, Eur. J. Echocardiogr. 10 (6) (2009) 738–744.

[23] H. Muller, H. Burri, R. Lerch, Evaluation of right atrial size in patients with atrial arrhythmias: comparison of 2D versus real time 3D echocardiography, Echocardiography 25 (6) (2008) 617–623.

[24] D. Peluso, L.P. Badano, D. Muraru, et al., Right atrial size and function assessed with three-dimensional and speckle-tracking echocardiography in 200 healthy volunteers, Eur. Heart J. Cardiovasc. Imaging 14 (11) (2013) 1106–1114.

[25] X. Zhao, J.M. Zhang, J.A. Bryant, et al., Elevated right atrial pressure associated with alteration of left ventricular contractility and ventricular-arterial coupling in pulmonary artery hypertension, Annu. Int. Conf. IEEE Eng. Med. Biol. Soc. 2019 (2019) 820–823.

[26] R. Manczak, M. Kurzyna, M. Pilka, et al., Prediction of prognostic hemodynamic indices in pulmonary hypertension using non-invasive parameters, Diagnostics (Basel) 10 (9) (2020).

[27] M. Obokata, G.C. Kane, H. Sorimachi, et al., Noninvasive evaluation of pulmonary artery pressure during exercise: the importance of right atrial hypertension, Eur. Respir. J. 55 (2) (2020).

[28] R. Watanabe, H. Amano, F. Saito, et al., Echocardiographic surrogates of right atrial pressure in pulmonary hypertension, Heart Vessel. 34 (3) (2019) 477–483.

[29] P. de Groote, M. Delobelle, E. Hebbar, et al., Right heart catheterization in advanced systolic heart failure. What are the most useful haemodynamic parameters for risk stratification? Arch. Cardiovasc. Dis. 115 (3) (2022) 169–178.

[30] T. Taniguchi, T. Ohtani, S. Nakatani, et al., Impact of body size on inferior vena cava parameters for estimating right atrial pressure: a need for standardization? J. Am. Soc. Echocardiogr. 28 (12) (2015) 1420–1427.

[31] T. Kawata, M. Daimon, K. Nakanishi, et al., Factors influencing inferior vena cava diameter and its respiratory variation: simultaneous comparison with hemodynamic data, J. Cardiol. 79 (5) (2022) 642–647.

[32] C. Mitchell, P.S. Rahko, L.A. Blauwet, et al., Guidelines for performing a comprehensive transthoracic echocardiographic examination in adults: recommendations from the American Society of Echocardiography, J. Am. Soc. Echocardiogr. 32 (1) (2019) 1–64.

[33] M. Murayama, S. Kaga, K. Okada, et al., Clinical utility of superior vena cava flow velocity waveform measured from the subcostal window for estimating right atrial pressure, J. Am. Soc. Echocardiogr. 35 (7) (2022) 727–737.

[34] H. Utsunomiya, S. Nakatani, M. Nishihira, et al., Value of estimated right ventricular filling pressure in predicting cardiac events in chronic pulmonary arterial hypertension, J. Am. Soc. Echocardiogr. 22 (12) (2009) 1368–1374.

[35] Y. Hayabuchi, M. Sakata, T. Ohnishi, M. Inoue, S. Kagami, Ratio of early diastolic tricuspid inflow to tricuspid lateral annulus velocity reflects pulmonary regurgitation severity but not right ventricular diastolic function in children with repaired tetralogy of fallot, Pediatr. Cardiol. 34 (5) (2013) 1112–1117.

[36] R.S. Tsutsui, A. Borowski, W.H. Tang, J.D. Thomas, Z.B. Popovic, Precision of echocardiographic estimates of right atrial pressure in patients with acute decompensated heart failure, J. Am. Soc. Echocardiogr. 27 (10) (2014) 1072–1078, e1072.

[37] S. Frea, P. Centofanti, S. Pidello, et al., Noninvasive assessment of hemodynamic status in HeartWare left ventricular assist device patients: validation of an echocardiographic approach, JACC Cardiovasc. Imaging 12 (7 Pt 1) (2019) 1121–1131.

[38] J.B. Ivey-Miranda, E.L. Posada-Martinez, E. Almeida-Gutierrez, E. Flores-Umanzor, G. Borrayo-Sanchez, G. Saturno-Chiu, Assessment of right atrial pressure with two-dimensional, doppler and speckle tracking echocardiography in patients with acute right ventricular myocardial infarction, Med. Intens. (Engl. Ed.) 43 (7) (2019) 444–446.

[39] K. Said, A. Shehata, Z. Ashour, S. El-Tobgi, Value of conventional and tissue doppler echocardiography in the noninvasive measurement of right atrial pressure, Echocardiography. 29 (7) (2012) 779–784.

[40] O. Yildirimturk, Y. Tayyareci, R. Erdim, et al., Assessment of right atrial pressure using echocardiography and correlation with catheterization, J. Clin. Ultrasound 39 (6) (2011) 337–343.

[41] A.J. Fletcher, S. Robinson, B.S. Rana, Echocardiographic RV-E/e' for predicting right atrial pressure: a review, Echo Res Pract. 7 (4) (2020) R11–R20.

[42] E. Ostenfeld, A. Werther-Evaldsson, H. Engblom, et al., Discriminatory ability of right atrial volumes with two- and three-dimensional echocardiography to detect elevated right atrial pressure in pulmonary hypertension, Clin. Physiol. Funct. Imaging 38 (2) (2018) 192–199.

[43] A. Nemes, A. Kormanyos, P. Domsik, A. Kalapos, N. Ambrus, C. Lengyel, Normal reference values of three-dimensional speckle-tracking echocardiography-derived right atrial volumes and volume-based functional properties in healthy adults (Insights from the MAGYAR-healthy Study), J. Clin. Ultrasound 48 (5) (2020) 263–268.

[44] L. Thomas, M. Hoy, K. Byth, N.B. Schiller, The left atrial function index: a rhythm independent marker of atrial function, Eur. J. Echocardiogr. 9 (3) (2008) 356–362.

[45] S.A. Mouratoglou, K. Dimopoulos, V. Kamperidis, et al., Right atrial function predicts clinical outcome in patients with precapillary pulmonary hypertension, J. Am. Soc. Echocardiogr. 31 (10) (Oct 2018) 1137–1145.

[46] L.P. Badano, T.J. Kolias, D. Muraru, et al., Standardization of left atrial, right ventricular, and right atrial deformation imaging using two-dimensional speckle tracking echocardiography: a consensus document of the EACVI/ASE/Industry task force to standardize deformation imaging, Eur. Heart J. Cardiovasc. Imaging 19 (6) (2018) 591–600.

[47] J.U. Voigt, G. Pedrizzetti, P. Lysyansky, et al., Definitions for a common standard for 2D speckle tracking echocardiography: consensus document of the EACVI/ASE/industry task force to standardize deformation imaging, J. Am. Soc. Echocardiogr. 28 (2) (2015) 183–193.

[48] K. Haji, T.H. Marwick, Clinical utility of echocardiographic strain and strain rate measurements, Curr. Cardiol. Rep. 23 (3) (2021) 18.

[49] A. Opdahl, T. Helle-Valle, H. Skulstad, O.A. Smiseth, Strain, strain rate, torsion, and twist: echocardiographic evaluation, Curr. Cardiol. Rep. 17 (3) (2015) 568.

[50] A. Stoylen, A. Heimdal, K. Bjornstad, H.G. Torp, T. Skjaerpe, Strain rate imaging by ultrasound in the diagnosis of regional dysfunction of the left ventricle, Echocardiography 16 (4) (1999) 321–329.

[51] O. Gjesdal, T. Helle-Valle, E. Hopp, et al., Noninvasive separation of large, medium, and small myocardial infarcts in survivors of reperfused ST-elevation myocardial infarction: a comprehensive tissue Doppler and speckle-tracking echocardiography study, Circ Cardiovasc Imaging 1 (3) (2008) 189–196, 182 p following 196.

[52] D. Genovese, A. Singh, V. Volpato, et al., Load dependency of left atrial strain in normal subjects, J. Am. Soc. Echocardiogr. 31 (11) (2018) 1221–1228.

[53] A. Hosseinsabet, R. Mahmoudian, A. Jalali, R. Mohseni-Badalabadi, T. Davarpasand, Normal ranges of right atrial strain and strain rate by two-dimensional speckle-tracking echocardiography: a systematic review and meta-analysis, Front. Cardiovasc. Med. 8 (2021), 771647.

[54] O. Mirea, E.D. Pagourelias, J. Duchenne, et al., Variability and reproducibility of segmental longitudinal strain measurement: a report from the EACVI-ASE strain standardization task force, JACC Cardiovasc. Imaging 11 (1) (2018) 15–24.

[55] A. Nemes, I. Marton, P. Domsik, et al., The right atrium in idiopathic hypereosinophilic syndrome : insights from the 3D speckle tracking echocardiographic MAGYAR-path study, Herz 44 (5) (Aug 2019) 405–411.

[56] A. Nemes, P. Domsik, A. Kalapos, H. Gavaller, M. Oszlanczi, T. Forster, Right atrial deformation analysis in isolated left ventricular noncompaction - insights from the three-dimensional speckle tracking echocardiographic MAGYAR-path study, Rev. Port. Cardiol. 35 (10) (Oct 2016) 515–521.

[57] A. Nemes, D. Foldeak, P. Domsik, et al., Right atrial deformation analysis in cardiac amyloidosis - results from the three-dimensional speckle-tracking echocardiographic MAGYAR-path study, Arq. Bras. Cardiol. 111 (3) (Sep 2018) 384–391.

[58] A. Nemes, K. Havasi, P. Domsik, A. Kalapos, T. Forster, Evaluation of right atrial dysfunction in patients with corrected tetralogy of fallot using 3D speckle-tracking echocardiography. Insights from the CSONGRAD registry and MAGYAR-path study, Herz 40 (7) (Nov 2015) 980–988.

[59] A. Nemes, P. Domsik, A. Kalapos, A. Kormanyos, N. Ambrus, T. Forster, Three-dimensional speckle-tracking echocardiography detects different patterns of right atrial dysfunction in selected disorders: a short summary from the MAGYAR-path study, Quant. Imaging Med. Surg. 8 (2) (2018) 182–186.

[60] M. Padeletti, M. Cameli, M. Lisi, A. Malandrino, V. Zaca, S. Mondillo, Reference values of right atrial longitudinal strain imaging by two-dimensional speckle tracking, Echocardiography 29 (2) (2012) 147–152.

[61] A. Nemes, A. Kormanyos, P. Domsik, et al., Normal reference values of right atrial strain parameters using three-dimensional speckle-tracking echocardiography (results from the MAGYAR-healthy Study), Int. J. Cardiovasc. Imaging 35 (11) (2019) 2009–2018.

[62] A. Nemes, A. Kormanyos, P. Domsik, A. Kalapos, C. Lengyel, T. Forster, Normal reference values of three-dimensional speckle-tracking echocardiography-derived left atrial strain parameters (results from the MAGYAR-healthy Study), Int. J. Cardiovasc. Imaging 35 (6) (2019) 991–998.

[63] S. Moustafa, H. Zuhairy, M.A. Youssef, et al., Right and left atrial dissimilarities in Normal subjects explored by speckle tracking echocardiography, Echocardiography 32 (9) (2015) 1392–1399.

[64] F. Alenezi, S. Rajagopal, S. Kutty, Assessing right atrial function in pulmonary hypertension: window to the soul of the right heart? Am. J. Physiol. Heart Circ. Physiol. 318 (1) (2020) H154–H155.

[65] N.E. Hasselberg, N. Kagiyama, Y. Soyama, et al., The prognostic value of right atrial strain imaging in patients with precapillary pulmonary hypertension, J. Am. Soc. Echocardiogr. 34 (8) (2021) 851–861, e851.

[66] P. Lancellotti, L. Moura, L.A. Pierard, et al., European Association of Echocardiography recommendations for the assessment of valvular regurgitation. Part 2: mitral and tricuspid regurgitation (native valve disease), Eur. J. Echocardiogr. 11 (4) (May 2010) 307–332.

[67] A.C. To, S.D. Flamm, T.H. Marwick, A.L. Klein, Clinical utility of multimodality LA imaging: assessment of size, function, and structure, JACC Cardiovasc. Imaging 4 (7) (Jul 2011) 788–798.

[68] M. Sareban, T. Perz, F. Macholz, et al., Preserved right ventricular function but increased right atrial contractile demand in altitude-induced pulmonary hypertension, Int. J. Cardiovasc. Imaging 36 (6) (2020) 1069–1076.

[69] M.J. Richter, F. Fortuni, M.A. Wiegand, et al., Association of right atrial conduit phase with right ventricular lusitropic function in pulmonary hypertension, Int. J. Cardiovasc. Imaging 36 (4) (2020) 633–642.

[70] W. Liu, Y. Wang, J. Zhou, H. Bai, F. Wang, J. Wang, The association of functional capacity with right atrial deformation in patients with pulmonary arterial hypertension: a study with two-dimensional speckle tracking, Heart Lung Circ. 27 (3) (2018) 350–358.

[71] T. Sato, I. Tsujino, N. Oyama-Manabe, et al., Right atrial volume and phasic function in pulmonary hypertension, Int. J. Cardiol. 168 (1) (2013) 420–426.

[72] S.L. Gaynor, H.S. Maniar, S.M. Prasad, P. Steendijk, M.R. Moon, Reservoir and conduit function of right atrium: impact on right ventricular filling and cardiac output, Am. J. Physiol. Heart Circ. Physiol. 288 (5) (2005) H2140–H2145.

[73] F. Alenezi, A. Mandawat, Z.J. Il'Giovine, et al., Clinical utility and prognostic value of right atrial function in pulmonary hypertension, Circ. Cardiovasc. Imaging 11 (11) (2018), e006984.

[74] N.M. Bhave, S.H. Visovatti, B. Kulick, T.J. Kolias, V.V. McLaughlin, Right atrial strain is predictive of clinical outcomes and invasive hemodynamic data in group 1 pulmonary arterial hypertension, Int. J. Cardiovasc. Imaging. 33 (6) (2017) 847–855.

[75] T. Sato, I. Tsujino, H. Ohira, et al., Right atrial volume and reservoir function are novel independent predictors of clinical worsening in patients with pulmonary hypertension, J Heart Transplant. 34 (3) (2015) 414–423.

[76] K. Darsaklis, M.E. Dickson, W. Cornwell 3rd, et al., Right atrial emptying fraction non-invasively predicts mortality in pulmonary hypertension, Int. J. Cardiovasc. Imaging 32 (7) (2016) 1121–1130.

[77] J.A. Goldstein, Hemodynamic complications of right ventricular infarction: role of the right atrium, JACC Case Rep. 3 (9) (2021) 1174–1176.

[78] B.G. Kanar, M. Sunbul, A.A. Sahin, Z. Dogan, M.K. Tigen, Evaluation of right atrial volumes and functions by real-time three-dimensional echocardiography in patients after acute inferior myocardial infarction, Echocardiography. 35 (11) (2018) 1806–1811.

[79] S. Nourian, A. Hosseinsabet, A. Jalali, R. Mohseni-Badalabadi, Evaluation of right atrial function by two-dimensional speckle-tracking echocardiography in patients with right ventricular myocardial infarction, Int J Cardiovasc Imaging. 33 (1) (2017) 47–56.

[80] E.H. Cushing, H.S. Feil, E.J. Stanton, W.B. Wartman, Infarction of the cardiac auricles (Atria): clinical, pathological, and experimental studies, Br. Heart J. 4 (1–2) (1942) 17–34.

[81] M.L. Lu, T. De Venecia, S. Patnaik, V.M. Figueredo, Atrial myocardial infarction: a tale of the forgotten chamber, Int. J. Cardiol. 202 (2016) 904–909.

[82] A. Hosseinsabet, M. Salarifar, Right atrial appendage thrombosis in a patient with a history of myocardial infarction, J. Cardiovasc. Echogr. 31 (1) (2021) 55–56.

[83] A. Frustaci, C. Chimenti, F. Bellocci, E. Morgante, M.A. Russo, A. Maseri, Histological substrate of atrial biopsies in patients with lone atrial fibrillation, Circulation 96 (4) (1997) 1180–1184.

[84] C.F.T. Aimé-Sempé, C. Rücker-Martin, et al., Myocardial cell death in fibrillating and dilated human right atria, J. Am. Coll. Cardiol. 34 (35) (1999) 1577–1586.

[85] N. Li, B. Brundel, Inflammasomes and proteostasis novel molecular mechanisms associated with atrial fibrillation, Circ. Res. 127 (1) (2020) 73–90.

[86] D. Qiu, L. Peng, D.N. Ghista, K.K.L. Wong, Left atrial remodeling mechanisms associated with atrial fibrillation, Cardiovasc. Eng. Technol. 12 (3) (2021) 361–372.

[87] L.P.S.M. Lai, J.L. Lin, et al., Down-regulation of L-type calcium channel and sarcoplasmic reticular Ca(2+)-ATPase mRNA in human atrial fibrillation without significant change in the mRNA of ryanodine receptor, calsequestrin and phospholamban: an insight into the mechanism of atrial electrical remodeling, J. Am. Coll. Cardiol. 33 (35) (1999) 1231–1237.

[88] J. Liao, S. Zhang, S. Yang, et al., Interleukin-6-mediated-Ca(2+) handling abnormalities contributes to atrial fibrillation in sterile pericarditis rats, Front. Immunol. 12 (2021), 758157.

[89] F. Reinhardt, K. Beneke, N.G. Pavlidou, et al., Abnormal calcium handling in atrial fibrillation is linked to changes in cyclic AMP dependent signaling, Cells. 10 (11) (2021).

[90] S. Prabhu, A. Voskoboinik, A.J.A. McLellan, et al., A comparison of the electrophysiologic and electroanatomic characteristics between the right and left atrium in persistent atrial fibrillation: is the right atrium a window into the left? J. Cardiovasc. Electrophysiol. 28 (10) (2017) 1109–1116.

[91] Y. Akutsu, K. Kaneko, Y. Kodama, et al., Association between left and right atrial remodeling with atrial fibrillation recurrence after pulmonary vein catheter ablation in patients with paroxysmal atrial fibrillation: a pilot study, Circ. Cardiovasc. Imaging. 4 (5) (2011) 524–531.

[92] S.K. Therkelsen, B.A. Groenning, J.H. Svendsen, G.B. Jensen, Atrial and ventricular volume and function evaluated by magnetic resonance imaging in patients with persistent atrial fibrillation before and after cardioversion, Am. J. Cardiol. 97 (8) (2006) 1213–1219.

[93] L. Soulat-Dufour, S. Lang, S. Ederhy, et al., Biatrial remodelling in atrial fibrillation: a three-dimensional and strain echocardiography insight, Arch Cardiovasc. Dis. 112 (10) (2019) 585–593.

[94] M. Govindan, A. Kiotsekoglou, S.K. Saha, A.J. Camm, Right atrial myocardial deformation by two-dimensional speckle tracking echocardiography predicts recurrence in paroxysmal atrial fibrillation, J. Echocardiogr. 15 (4) (2017) 166–175.

[95] U. Aksu, K. Kalkan, O. Gulcu, E. Aksakal, M. Ozturk, S. Topcu, The role of the right atrium in development of postoperative atrial fibrillation: a speckle tracking echocardiography study, J. Clin. Ultrasound 47 (8) (2019) 470–476.

[96] A.C. Guta, L.P. Badano, M. Tomaselli, et al., The pathophysiological link between right atrial remodeling and functional tricuspid regurgitation in patients with atrial fibrillation: a three-dimensional echocardiography study, J. Am. Soc. Echocardiogr. 34 (6) (2021) 585–594, e581.

[97] D. Muraru, S. Caravita, A.C. Guta, et al., Functional tricuspid regurgitation and atrial fibrillation: which comes first, the chicken or the egg? CASE (Phila) 4 (5) (2020) 458–463.

[98] X.A. Ortiz-Leon, E.L. Posada-Martinez, M.C. Trejo-Paredes, et al., Understanding tricuspid valve remodelling in atrial fibrillation using three-dimensional echocardiography, Eur. Heart J. Cardiovasc. Imaging 21 (7) (2020) 747–755.

[99] S. Fukuda, G. Saracino, Y. Matsumura, et al., Three-dimensional geometry of the tricuspid annulus in healthy subjects and in patients with functional tricuspid regurgitation: a real-time, 3-dimensional echocardiographic study, Circulation 114 (1 Suppl) (2006) I492–I498.

[100] A.M. Anwar, M.L. Geleijnse, O.I. Soliman, et al., Assessment of normal tricuspid valve anatomy in adults by real-time three-dimensional echocardiography, Int. J. Cardiovasc. Imaging. 23 (6) (2007) 717–724.

[101] K. Addetia, D. Muraru, F. Veronesi, et al., 3-dimensional echocardiographic analysis of the tricuspid annulus provides new insights into tricuspid valve geometry and dynamics, JACC Cardiovasc. Imaging 12 (3) (2019) 401–412.

[102] O.K. Khalique, J.L. Cavalcante, D. Shah, et al., Multimodality imaging of the tricuspid valve and right heart anatomy, JACC Cardiovasc. Imaging 12 (3) (2019) 516–531.

[103] E.A. Prihadi, V. Delgado, R.T. Hahn, R. Leipsic, J.K. Min, J.J. Bax, Imaging needs in novel transcatheter tricuspid valve interventions, JACC Cardiovasc. Imaging 11 (5) (2018) 736–754.

[104] D. Muraru, A.C. Guta, R.C. Ochoa-Jimenez, et al., Functional regurgitation of atrioventricular valves and atrial fibrillation: an elusive pathophysiological link deserving further attention, J. Am. Soc. Echocardiogr. 33 (1) (2020) 42–53.

[105] N. Yamasaki, F. Kondo, T. Kubo, et al., Severe tricuspid regurgitation in the aged: atrial remodeling associated with long-standing atrial fibrillation, J. Cardiol. 48 (6) (2006) 315–323.

[106] D. Muraru, K. Addetia, A.C. Guta, et al., Right atrial volume is a major determinant of tricuspid annulus area in functional tricuspid regurgitation: a three-dimensional echocardiographic study, Eur. Heart J. Cardiovasc. Imaging 22 (6) (2021) 660–669.

[107] H. Utsunomiya, Y. Itabashi, H. Mihara, et al., Functional tricuspid regurgitation caused by chronic atrial fibrillation: a real-time 3-dimensional transesophageal echocardiography study, Circ. Cardiovasc. Imaging. 10 (1) (2017).

[108] M.Q. Najib, K.L. Vinales, S.S. Vittala, S. Challa, H.R. Lee, H.P. Chaliki, Predictors for the development of severe tricuspid regurgitation with anatomically normal valve in patients with atrial fibrillation, Echocardiography 29 (2) (2012) 140–146.

[109] N. Nemoto, J.R. Lesser, W.R. Pedersen, et al., Pathogenic structural heart changes in early tricuspid regurgitation, J. Thorac. Cardiovasc. Surg. 150 (2) (Aug 2015) 323–330.

[110] Y. Topilsky, S. Maltais, J. Medina Inojosa, et al., Burden of tricuspid regurgitation in patients diagnosed in the community setting, JACC Cardiovasc. Imaging 12 (3) (2019) 433–442.

[111] J. Afilalo, J. Grapsa, P. Nihoyannopoulos, et al., Leaflet area as a determinant of tricuspid regurgitation severity in patients with pulmonary hypertension, Circ. Cardiovasc. Imaging 8 (5) (2015).

[112] L.P. Badano, R. Hahn, H. Rodriguez-Zanella, D. Araiza Garaygordobil, R. C. Ochoa-Jimenez, D. Muraru, Morphological assessment of the tricuspid apparatus and grading regurgitation severity in patients with functional tricuspid regurgitation: thinking outside the box, JACC Cardiovasc. Imaging 12 (4) (2019) 652–664.

[113] H. Utsunomiya, Y. Harada, H. Susawa, et al., Tricuspid valve geometry and right heart remodelling: insights into the mechanism of atrial functional tricuspid regurgitation, Eur. Heart J. Cardiovasc. Imaging 21 (10) (2020) 1068–1078.

[114] M. Writing Committee, C.M. Otto, R.A. Nishimura, et al., 2020 ACC/AHA guideline for the management of patients with valvular heart disease: a report of the American College of Cardiology/American Heart Association Joint Committee on clinical practice guidelines, J. Am. Coll. Cardiol. 77 (4) (2021) e25–e197.

[115] V. Falk, H. Baumgartner, J.J. Bax, et al., 2017 ESC/EACTS guidelines for the management of valvular heart disease, Eur. J. Cardiothorac. Surg. 52 (4) (2017) 616–664.

[116] M. Taramasso, G. Benfari, P. van der Bijl, et al., Transcatheter versus medical treatment of patients with symptomatic severe tricuspid regurgitation, J. Am. Coll. Cardiol. 74 (24) (2019) 2998–3008.

[117] A. Vahanian, F. Beyersdorf, F. Praz, et al., 2021 ESC/EACTS guidelines for the management of valvular heart disease, Eur. J. Cardiothorac. Surg. 60 (4) (2021) 727–800.

[118] M. Writing Committee, C.M. Otto, R.A. Nishimura, et al., 2020 ACC/AHA guideline for the management of patients with valvular heart disease: executive summary: a report of the American College of Cardiology/American Heart Association Joint Committee on clinical practice guidelines, J. Am. Coll. Cardiol. 77 (4) (2021) 450–500.

[119] D.R. Florescu, D. Muraru, C. Florescu, et al., Right heart chambers geometry and function in patients with the atrial and the ventricular phenotypes of functional tricuspid regurgitation, Eur. Heart J. Cardiovasc. Imaging 23 (7) (2022) 930–940.

[120] F. Fortuni, M.F. Dietz, E.A. Prihadi, et al., Ratio between vena contracta width and tricuspid annular diameter: prognostic value in secondary tricuspid regurgitation, J. Am. Soc. Echocardiogr. 34 (9) (2021) 944–954.

[121] J. Wang, S. Li, Q. Ye, et al., Catheter ablation or surgical therapy in moderate-severe tricuspid regurgitation caused by long-standing persistent atrial fibrillation. Propensity score analysis, J. Cardiothorac. Surg. 15 (1) (2020) 277.

[122] K. Itakura, T. Hidaka, Y. Nakano, et al., Successful catheter ablation of persistent atrial fibrillation is associated with improvement in functional tricuspid regurgitation and right heart reverse remodeling, Heart Vessel. 35 (6) (2020) 842–851.